

# Rapid Laser Reactive Sintering for Sustainable and Clean Preparation of Protonic Ceramics

Shenglong Mu, Hua Huang, Akihiro Ishii, Yuzhe Hong, Aaron Santomauro, Zeyu Zhao, Minda Zou, Fei Peng, Kyle S. Brinkman, Hai Xiao, and Jianhua Tong\*



Cite This: *ACS Omega* 2020, 5, 11637–11642



Read Online

ACCESS |



Metrics & More

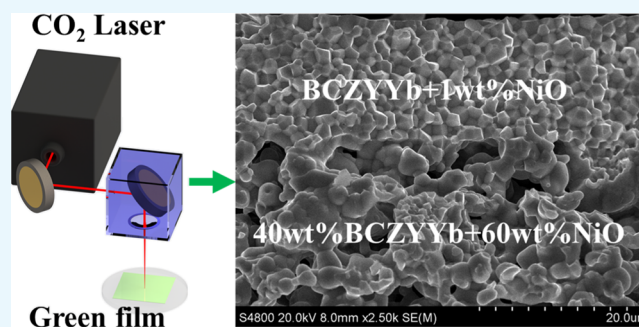


Article Recommendations



Supporting Information

**ABSTRACT:** One of the essential challenges for energy conversion and storage devices based on protonic ceramics is that the high temperature (1600–1700 °C) and long-time firing (>10 h) are inevitably required for the fabrication, which makes the sustainable and clean manufacturing of protonic ceramic devices impractical. This study provided a new rapid laser reactive sintering (RLRS) method for the preparation of nine protonic ceramics [i.e., BaZr<sub>0.8</sub>Y<sub>0.2</sub>O<sub>3-δ</sub> (BZY20), BZY20 + 1 wt % NiO, BaCe<sub>0.7</sub>Zr<sub>0.1</sub>Y<sub>0.1</sub>Yb<sub>0.1</sub>O<sub>3-δ</sub> (BCZYYb), BCZYYb + 1 wt % NiO, 40 wt % BCZYYb + 60 wt % NiO, BaCe<sub>0.85</sub>Fe<sub>0.15</sub>O<sub>3-δ</sub>–BaCe<sub>0.15</sub>Fe<sub>0.85</sub>O<sub>3-δ</sub> (BCF), BaCo<sub>0.4</sub>Fe<sub>0.4</sub>Zr<sub>0.1</sub>Y<sub>0.1</sub>O<sub>3-δ</sub> (BCFZY0.1), BaCe<sub>0.6</sub>Zr<sub>0.3</sub>Y<sub>0.1</sub>O<sub>3-δ</sub> (BCZY63), and La<sub>0.7</sub>Sr<sub>0.3</sub>CrO<sub>3-δ</sub> (LSC)] with desired crystal structures and microstructures. Following this, the dual-layer half-cells, comprising the porous electrode and dense electrolyte, were prepared by the developed RLRS technique. After applying the BCFZY0.1 cathode, the protonic ceramic fuel cell (PCFC) single cells were prepared and tested initially. The derived conductivity of the RLRS electrolyte films showed comparable proton conductivity with the electrolyte prepared by conventional furnace sintering. The initial cost estimation based on electricity consumption during the sintering process for the fabrication of PCFC single cells showed that RLRS is more competitive than the conventional furnace sintering. This RLRS can be combined with the rapid additive manufacturing of ceramics for the sustainable and clean manufacturing of protonic ceramic energy devices and the processing of other ceramic devices.



## INTRODUCTION

The refractory nature of ceramics is beneficial to use them as structural materials; however, it is sometimes recognized as an encumbrance, when using them as functional materials. A typical case is the protonic ceramics used for energy conversion and storage devices (e.g., fuel cells, electrolyzers, membrane reactors).<sup>1–4</sup> The electrolyte and interconnect involved in protonic ceramic energy devices require to be fired at temperatures as high as 1700 °C for longer than 10 h to achieve high relative density.<sup>5–8</sup> This high-temperature and long-time processes have been abhorred, not only for its energy and time consumptions but also for the volatilization of the materials, leading to the poor performance.<sup>9</sup> Moreover, when fabricating the devices (i.e., single cells and stacks), the refractory nature becomes a more severe problem because the dense electrolyte and interconnect must be integrated with the porous electrode layers, which need to have an excellent nanoporous structure for ensuring enough surface area for excellent electrocatalytic fuel oxidation or oxygen reduction reactions.

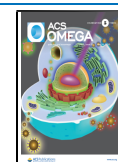
The conventional method for manufacturing protonic ceramics with desired crystal structures and microstructures is described by route 1 in Figure 1. The primary four steps of

(a) mixing raw powders of each material by ball milling, (b) calcination of each material, (c) shape formation by pelletizing (bulks) or tape casting (films), and (d) sintering are needed. The calcination step usually is performed at a temperature higher than 900 °C for more than 10 h to obtain phase-pure ceramic powders.<sup>10,11</sup> Sometimes, the particular wet-chemistry method is used to obtain pure-phase nanopowder for better controlling the microstructure during sintering, which inevitably results in more expensive precursors and much longer preparation time (e.g., a week or so is needed to prepare fine BaZr<sub>0.8</sub>Y<sub>0.2</sub>O<sub>3-δ</sub> (BZY20) powder through the modified Pechini method).<sup>10–12</sup> The conventional sintering of protonic ceramics (e.g., BZY20) is performed at 1600–1700 °C for more than 10 h in a protecting powder bath, comprising of 90 wt % BZY20 and 10 wt % BaCO<sub>3</sub> under a pure oxygen atmosphere. However, the high-temperature sintering of

Received: February 27, 2020

Accepted: April 30, 2020

Published: May 14, 2020



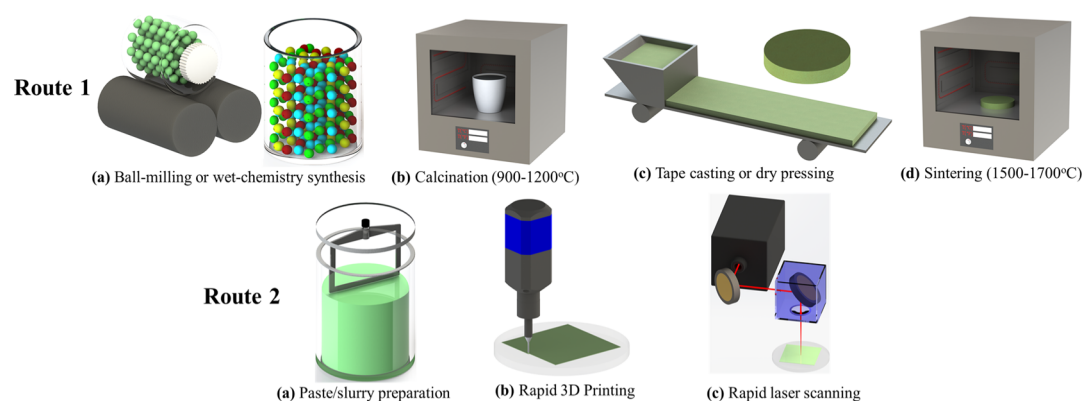


**Figure 1.** Schematic description of protonic ceramics. Route 1: Conventional ceramic-processing method and Route 2: Rapid laser reactive processing method.

**Table 1.** Laser Operation Parameters for Sintering Protonic Ceramic Components

|                     | BZY20 | BZY20 + 1 wt % NiO | BCZYYb | BCZYYb + 1 wt % NiO | 40 wt % BCZYYb + 60 wt % NiO | BCZY63 | BCFZY0.1 | LSC | BCF |
|---------------------|-------|--------------------|--------|---------------------|------------------------------|--------|----------|-----|-----|
| laser power (W)     | 7     | 7                  | 2.8    | 2.8                 | 100                          | 10     | 70       | 85  | 10  |
| moving speed (mm/s) | 1     | 1                  | 1      | 1                   | 0.2                          | 1      | 0.5      | 01  | 1   |
| defocus (mm)        | 20    | 20                 | 20     | 20                  | 30                           | 20     | no lens  | 20  | 10  |

BZY20 directly disqualified it for the preparation of single cells or half-cells for protonic ceramic devices. Several research groups investigated many promising ceramic sintering methods for densifying ceramics.<sup>12</sup> The primary purpose of these methods was to reduce the fabrication temperature, time, and cost. The two-step sintering was proven to be able to reduce the sintering time at peak temperature into several minutes, followed by a lower temperature step for some hours.<sup>13–16</sup> This method can reduce Ba loss and control the grain size while achieving the desired relative density at the same time.<sup>16</sup> Spark plasma sintering reduced the sintering time to several minutes by densifying the pellets in the die with the proper pressure and electric field.<sup>17</sup> Flash sintering is another promising ceramic sintering method, which can achieve high relative density within several seconds.<sup>18</sup> However, most of these sintering methods require specific equipment, high power consumption, and pressure assistance, which significantly limited the geometry flexibility of the sintered ceramics.<sup>19,20</sup> Recently, the solid-state reactive sintering (SSRS) has been discovered by Tong et al., which allows the fabrication of protonic ceramics, even single cells/half-cells in one-step with the help of sintering aids while sintering at a moderate temperature (e.g., 1400–1500 °C). However, the long-term sintering at least 12 h must be satisfied for achieving the desired crystal structure and microstructure.<sup>21</sup> Furthermore, the SSRS method still has to face the challenge of integrating a fully densified electrolyte or interconnect with porous electrodes.<sup>22</sup>

In our previous work, a rapid laser reactive sintering (RLRS) technique was initially discovered for rapid sintering 3D-printed electrolyte green layers of protonic ceramic electrolytes, BZY20 and BCZYYb,<sup>9</sup> into dense films to develop integrated additive manufacturing and laser processing of protonic ceramic electrolyzer stacks. The combination of rapid heating and instant solid state reaction allowed the fast phase formation and the densification of BZY20 and BCZYYb. This

RLRS technique is schematically described by route 2 in Figure 1, which can be simply divided into three steps of paste preparation, 3D printing, and laser reactive sintering. A much more controllable and rapid 3D printing was added while the time and energy-consuming calcination and sintering steps were replaced by a fast and straightforward cost-effective laser scanning step.<sup>23</sup> In the present work, the RLRS technique was extensively used for processing the protonic ceramics of electrolytes, hydrogen electrodes, oxygen electrodes, oxygen/hydrogen electrode scaffolds, interconnects, and mixed conducting dual-phase composites for fulfilling the rapid integrated additive and laser processing of protonic ceramic energy devices sustainably and cleanly.<sup>24,25</sup> Not only the desired crystal structures but also the desired microstructures (e.g., fully dense or highly porous structures) were obtained by the RLRS method. The fabrication of half-cells and single cells was demonstrated. The conductivity of the electrolyte derived for the single cell measurement showed comparable values to those obtained by the furnace sintering method. The RLRS provided a corner-stone knowledge for rapid integrated additive manufacturing and laser processing of protonic ceramic energy devices and other ceramic devices.

## RESULTS AND DISCUSSION

The X-ray diffraction (XRD) patterns of all the protonic ceramic component films prepared by the RLRS method under the optimized laser operation condition, summarized in Table 1 (Experimental Section), are displayed in Figure 2. In general, although the interaction between the laser beam and the materials was only around several seconds, it was enough to form the desired crystal structures for all the samples. As for the BCZYYb, BCZYYb + 1 wt % NiO, BZY20, BZY20 + 1 wt % electrolytes, the LSC interconnect, the BCFZY0.1 electrode, and the BCZY63 electrode scaffold (the thin film of BCZY63 was deposited on the BCZYYb electrolyte pellet, which resulted in the existence of BCZYYb peaks), the phase-pure

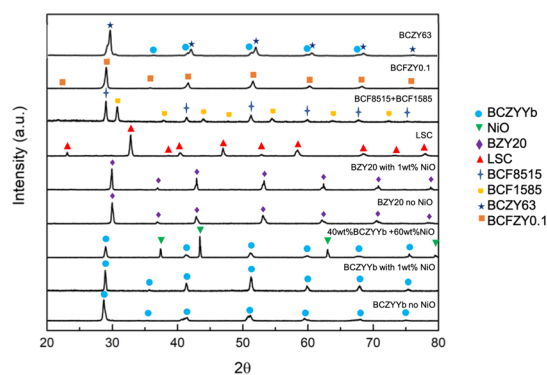


**Figure 2.** XRD patterns of the protonic ceramic component films obtained by the RLRS.

perovskite structure was obtained. Furthermore, the cermet hydrogen electrode based on BCZYYb electrolyte and NiO also showed the desired crystal structures of BCZYYb and NiO. There are no other peaks ascribed to impurities found. BCF is a complicated dual-phase material system comprising a cubic perovskite ( $\text{BaCe}_{0.85}\text{Fe}_{0.15}\text{O}_{3-\delta}$ , BCF8515) and an orthorhombic perovskite ( $\text{BaCe}_{0.15}\text{Fe}_{0.85}\text{O}_{3-\delta}$ , BCF1585) for using as a mixed protonic and electronic-conducting hydrogen permeation membrane, which usually is synthesized by using the modified Pechini method with extended processing time. Therefore, we can conclude that the RLRS method can achieve the desired crystal structure for extensive protonic ceramic component materials.

Figure 3 provides the SEM characterization of BCZYYb + 1 wt % electrolyte, BZY20 + 1 wt % NiO electrolyte, LSC

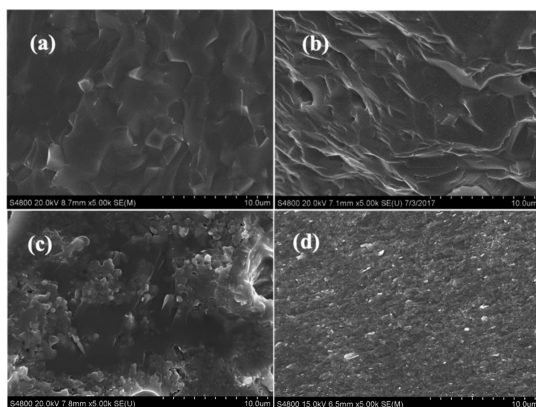


**Figure 3.** SEM images of dense protonic ceramic component films obtained by RLRS. (a) Cross-section of BCZYYb + 1 wt % NiO electrolyte film, (b) cross-section of BZY20 + 1 wt % NiO electrolyte film, (c) the cross-section of LSC interconnect film, and (d) the cross-section of BCF composite film.

interconnect, and BCF composite films obtained by RLRS. The cross-section image of the BCZYYb + 1 wt % NiO (Figure 3a) clearly shows that the electrolyte films were fully dense. The relative density analyzed by ImageJ based on multiple SEM images is high than 95%. The relatively large grain size was obtained, which will be significantly beneficial to the total proton conductivity of this film. Figure 3b indicates that the most refractory protonic ceramic electrolyte of BZY20 was fully densified with the help of 1 wt % of NiO sintering aid. The grain boundary was almost entirely removed by adjusting laser operating parameters. The relative density is around

98.9%. LSC is the state-of-the-art interconnect for solid oxide fuel cells, which, however, is very difficult to be densified too. For example, the sintering at 1550 °C for 10 h usually only gets a relative density of ~80% by the conventional method, as described in route 1 in Figure 1. Figure 3c provides the SEM image of the LSC after RLRS for a couple of seconds, from which it can be clearly seen that the LSC has been fully densified already. The relative density is around 98.7%. The BCF composite was recently reported to be a hydrogen-permeable membrane, comprising  $\text{BaCe}_{0.85}\text{Fe}_{0.15}\text{O}_{3-\delta}$  and  $\text{BaCe}_{0.15}\text{Fe}_{0.85}\text{O}_{3-\delta}$ ,<sup>14</sup> which usually needs to utilize the improved Pechini method to achieve the desired phase composite. Figure 3d shows that our newly developed RLRS method can fully densify the composite BCF films for hydrogen permeation. The BCF membrane showed a relative density of ~93%.

Figure 4 provides the SEM characterization results of porous protonic ceramic components of 40 wt % BCZYYb + 60 wt %

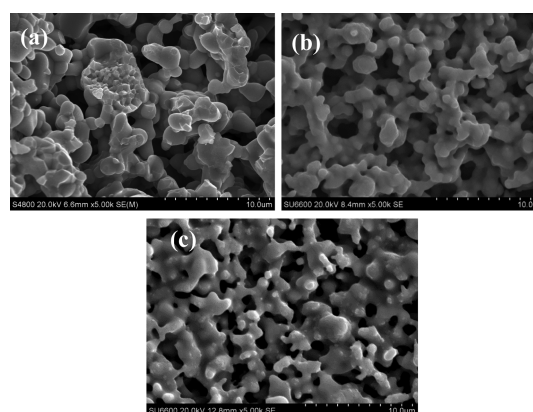


**Figure 4.** SEM images of the porous protonic ceramic components obtained by RLRS. (a) Cross-section of 40 wt % BCZYYb + 60 wt % NiO H<sub>2</sub> electrode film, (b) cross-section of BCZY63 O<sub>2</sub> electrode scaffold film, and (c) cross-section of BCFZY0.1 O<sub>2</sub> electrode film.

NiO hydrogen electrode, BCFZY0.1 oxygen electrode, and BCZY63 scaffold. It is evident that by optimizing the laser operation parameters, the highly porous microstructures of these three protonic ceramic component films were obtained successfully, which proved that the RLRS could also achieve porous protonic ceramic component films for working as the electrode or electrode scaffold.

Figure 5a further indicates that a half-cell comprising 40 wt % BCZYYb + 60 wt % NiO hydrogen electrode and a BCZYYb + 1 wt % NiO electrolyte was obtained by one-step laser scan, which proved that the RLRS could even make half-cells of the protonic ceramic device. Figure 5b shows that a defect-free half-cell with an active area of ~5 cm<sup>2</sup> was obtained. The

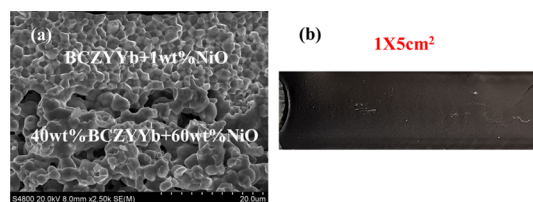


**Figure 5.** SEM image (a) and optical photo (b) of 40 wt % BCZYYb + 60 wt % NiO | BCZYYb + 1 wt % NiO half-cells.

obtained half-cell is nearly flat with less than a  $1^\circ$  angle curve-up from the side to the center.

The proton conductivity of the protonic ceramic is the essential property. We screen-printed a state-of-the-art cathode BCFZY0.1 on the top of an RLRS half-cell (BCZYYb + 1 wt% NiO | 40 wt % BCZYYb + 60 wt % NiO). Under open-circuit voltage conditions (air/ $H_2$ ), the ohmic resistance of the single cells and the conductivity were measured and calculated using the thickness obtained by SEM characterization after measurement. Figure 6 provides the proton conductivity of the

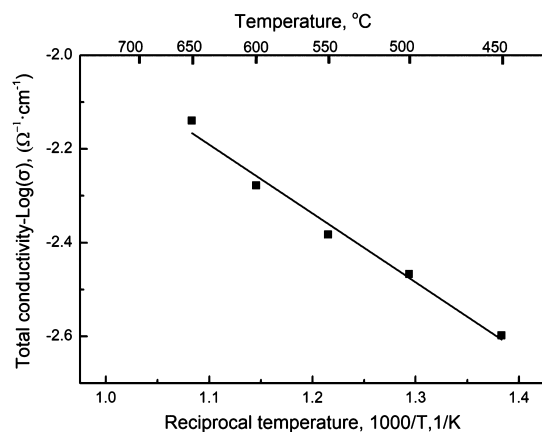


**Figure 6.** Conductivity of the BCZYYb electrolyte obtained by the RLRS method measured in the single cell operation under open-circuit voltage condition (air/ $H_2$  without humidification).

BCZYYb electrolyte at temperatures from 450 to 650 °C. The activation energy is around 30 kJ/mol, which is comparable to the one reported for protonic ceramics. The conductivity for the RLRS BCZYYb electrolyte is around  $5.3 \times 10^{-3}$  S/cm at 600 °C, which is also comparable to the one reported in the literature. Therefore, we can initially conclude that the RLRS method can obtain protonic ceramics with desired properties too.

The cost of the RLRS and the conventional furnace sintering method was initially compared based on the laboratory-scale fabrication of protonic ceramic fuel cell (PCFC) planar single cells. The cost was estimated mainly based on electricity consumption for fabricating twenty PCFC single cells with area  $10 \times 10$  cm<sup>2</sup>. For the RLRS, the electricity consumed by the CO<sub>2</sub> laser scanning of anode-supported electrolyte half-cells and the laser scanning of cathodes was included in the cost estimation. For conventional furnace sintering, the two temperature programs, described in Figure S1, were used to calculate the electricity consumption during the sintering process. The energy cost for the RLRS method is only ~34% of the energy cost for the conventional furnace sintering method. The detailed analysis is shown in the Supporting Information.

## CONCLUSIONS

The newly developed RLRS method was proven to be able to fabricate the electrolytes, electrodes, interconnect, gas-permeation composite, and half-cells for protonic ceramic energy devices with nine compositions. The XRD and SEM characterization showed that the desired crystal structures and microstructures for these protonic ceramic component films could be achieved. The initial conductivity measurement of protonic ceramic electrolytes prepared by RLRS showed

comparable values to those obtained by the furnace sintering method. The cost estimation based on the electricity consumption for the fabrication of PCFC single cells indicated that the RLRS method is more competitive than the conventional furnace sintering method. Therefore, the RLRS method can be used for the fabrication of protonic ceramics. The RLRS is expected to be able to rapidly sinter other ceramics with controllable microstructures, desired crystal structures, and properties. The instantaneous, controllable, and cost-effective advantages of the RLRS method allow it to be integrated with additive manufacturing for rapid processing of ceramics, which can open up a new avenue for advanced manufacturing of ceramics.

## EXPERIMENTAL SECTION

The state-of-the-art protonic ceramic components of dense electrolytes (BCZYYb + 1 wt % NiO, BCZYYb, BZY20 + 1 wt % NiO, and BZY20),<sup>9</sup> porous electrodes/electrode scaffolds [40 wt % BCZYYb + 60 wt % NiO, BaCe<sub>0.4</sub>Fe<sub>0.4</sub>Zr<sub>0.1</sub>Y<sub>0.1</sub>O<sub>3-δ</sub> (BCFZY0.1) BaCe<sub>0.6</sub>Zr<sub>0.3</sub>Y<sub>0.1</sub>O<sub>3-δ</sub> (BCZY63)],<sup>26,27</sup> dense interconnect (La<sub>0.7</sub>Sr<sub>0.3</sub>CrO<sub>3-δ</sub>/LSC),<sup>7</sup> and dense mixed protonic and electronic-conduction composite (BaCe<sub>0.85</sub>Fe<sub>0.15</sub>O<sub>3-δ</sub>-BaCe<sub>0.15</sub>Fe<sub>0.85</sub>O<sub>3-δ</sub>/BCF)<sup>28</sup> were chosen as model materials for the study of the RLRS processing of protonic ceramics. Green pastes of these protonic ceramic component precursors were prepared by ball-milling the raw materials of oxide and carbonate powders [e.g., BaCO<sub>3</sub> (Alfa Aesar 99.8%), Fe<sub>2</sub>O<sub>3</sub> (Alfa Aesar 99.9%), CeO<sub>2</sub> (Alfa Aesar 99.9%), ZrO<sub>2</sub> (Alfa Aesar 99.7%), La<sub>2</sub>O<sub>3</sub> (Alfa Aesar 99.9%), Cr<sub>2</sub>O<sub>3</sub> (Alfa Aesar 99%), SrCO<sub>3</sub> (Alfa Aesar 99.9%), NiO (Alfa Aesar Ni 78.5%), Y<sub>2</sub>O<sub>3</sub> (Alfa Aesar 99.9%), and Yb<sub>2</sub>O<sub>3</sub> (Alfa Aesar 99.9%)] for 48 h in the stoichiometric ratio, followed by mixing of the ball-milled powder with water, dispersant, and binder, as reported in ref 9. The green films of the component precursors were prepared either by microextrusion-based 3D printed or simple drop-coating on substrates of alumina plates and<sup>9,29</sup> fused silica or sintered the BCZYYb electrolyte pellet. The thin films with a usual thickness of ~150 μm were deposited and dried in the ambient atmosphere for 24 h. The CO<sub>2</sub> laser (Firestar TI100, wavelength 10.6 μm) was used to perform the RLRS. The laser was scanned across the green films by placing the films on a 3D-printing stage with X-Y motions to control scan speed and a Z-direction motion to control the degree of laser beam focus. The detailed laser operation parameters of laser power, scanning speed, and defocus distance are summarized in Table 1 for each protonic ceramic component film.

The crystal structure of each protonic ceramic component film prepared by RLRS was characterized by XRD (Rigaku Ultima IV). The laser-irradiated films were ground into powder. The XRD patterns were obtained by monochromatic Cu Kα radiation from 20 to 80° with 1°/min. The microstructures of representative protonic ceramic component films were observed by a scanning electron microscope (SEM, Hitachi S4800, Hitachi, Ltd., Tokyo, Japan).

The relative densities of the protonic ceramics were analyzed from multiple SEM images using the ImageJ software. The SEM images were imported into the ImageJ software for relative density calculation. By changing the black/white contrast (threshold) of the images, the pores can be automatically identified with significant color/contrast difference to the crystal grain/dense area. By counting the pixels of the areas of the pores and grains, we calculated the percentage

of the pores and then relative densities. Each sample's relative density was measured by this method five times to achieve average values.

In this work, the proton conductivities for the cell prepared using RLRS were analyzed by electrochemical impedance spectroscopy of the single cells. The half-cell was achieved by one-step sintering of the 3D-printed 40 wt % BCZYYb + 60 wt % NiO as the anode layer and spray-coating the BCZYYb electrolyte layer together. Then, the BCFZY0.1 cathode layer was screen-printed on the electrolyte surface of the half-cells fabricated by the RLRS method. The silver paste was applied to the two electrodes as current collectors. Silver wires were used to extend electrodes to the external conducting wires. Gamry Reference 600 plus was used for electrochemical impedance data recording with a perturbation voltage of 10 mV in the frequency range of 0.005 Hz to 5 MHz at temperatures of 450–650 °C, under open-circuit voltage conditions with UHP air (150 mL/min) on the cathode side and UHP H<sub>2</sub> (20 mL/min) on the anode side without prehumidification.

## ■ ASSOCIATED CONTENT

### Supporting Information

The Supporting Information is available free of charge at <https://pubs.acs.org/doi/10.1021/acsomega.0c00879>.

Rough estimation of electricity consumption for manufacturing PCFCs and the temperature programs for the fabrication of PCFC single cells using conventional furnace sintering methods (PDF)

## ■ AUTHOR INFORMATION

### Corresponding Author

Jianhua Tong – Department of Materials Science and Engineering, Clemson University, Clemson, South Carolina 29634, United States; [orcid.org/0000-0002-0684-1658](https://orcid.org/0000-0002-0684-1658); Email: [jianhut@clemson.edu](mailto:jianhut@clemson.edu)

### Authors

Shenglong Mu – Department of Materials Science and Engineering, Clemson University, Clemson, South Carolina 29634, United States

Hua Huang – Department of Materials Science and Engineering, Clemson University, Clemson, South Carolina 29634, United States

Akihiro Ishii – Department of Materials Science and Engineering, Clemson University, Clemson, South Carolina 29634, United States; [orcid.org/0000-0003-3858-2731](https://orcid.org/0000-0003-3858-2731)

Yuzhe Hong – Department of Materials Science and Engineering, Clemson University, Clemson, South Carolina 29634, United States

Aaron Santomauro – Department of Materials Science and Engineering, Clemson University, Clemson, South Carolina 29634, United States

Zeyu Zhao – Department of Materials Science and Engineering, Clemson University, Clemson, South Carolina 29634, United States

Minda Zou – Department of Materials Science and Engineering, Clemson University, Clemson, South Carolina 29634, United States

Fei Peng – Department of Materials Science and Engineering, Clemson University, Clemson, South Carolina 29634, United States; [orcid.org/0000-0002-3924-9028](https://orcid.org/0000-0002-3924-9028)

Kyle S. Brinkman – Department of Materials Science and Engineering, Clemson University, Clemson, South Carolina 29634, United States; [orcid.org/0000-0002-2219-1253](https://orcid.org/0000-0002-2219-1253)

Hai Xiao – Department of Electrical and Computer Engineering, Clemson University, Clemson, South Carolina 29634, United States

Complete contact information is available at: <https://pubs.acs.org/10.1021/acsomega.0c00879>

## Notes

The authors declare no competing financial interest.

This report was prepared as an account of work sponsored by an agency of the United States Government. Neither the United States Government nor any agency thereof, nor any of their employees, makes any warranty, express or implied, or assumes any legal liability or responsibility for the accuracy, completeness, or usefulness of any information, apparatus, product, or process disclosed, or represents that its use would not infringe privately owned rights. Reference herein, to any specific commercial product, process, or service by trade name, trademark, manufacturer, or otherwise does not necessarily constitute or imply its endorsement, recommendation, or favoring by the United States Government or any agency, thereof. The views and opinions of the authors expressed herein do not necessarily state or reflect those of the United States Government or any agency, thereof.

## ■ ACKNOWLEDGMENTS

This material is based upon work supported by the U.S. Department of Energy's Office of Energy Efficiency and Renewable Energy (EERE) under the Fuel Cell Technologies Office award number DE-EE0008428.

## ■ REFERENCES

- (1) Kochetova, N.; Animitsa, I.; Medvedev, D.; Demin, A.; Tsiakaras, P. Recent activity in the development of proton-conducting oxides for high-temperature applications. *RSC Adv.* **2016**, *6*, 73222–73268.
- (2) Yamazaki, Y.; Hernandez-Sanchez, R.; Haile, S. M. High total proton conductivity in large-grained yttrium-doped barium zirconate. *Chem. Mater.* **2009**, *21*, 2755–2762.
- (3) Shang, M.; Tong, J.; O'Hayre, R. A promising cathode for intermediate temperature protonic ceramic fuel cells: BaCo<sub>0.4</sub>Fe<sub>0.4</sub>Zr<sub>0.2</sub>O<sub>3-δ</sub>. *RSC Adv.* **2013**, *3*, 15769–15775.
- (4) Yang, L.; Wang, S.; Blinn, K.; Liu, M.; Liu, Z.; Cheng, Z.; Liu, M. Enhanced sulfur and coking tolerance of a mixed ion conductor for SOFCs: BaZr<sub>0.1</sub>Ce<sub>0.7</sub>Y<sub>0.2-x</sub>Yb<sub>x</sub>O<sub>3-δ</sub>. *Science* **2009**, *326*, 126–129.
- (5) Babilo, P.; Uda, T.; Haile, S. M. *J. Mater. Res.* **2007**, *22*, 1322–1330.
- (6) Kreuer, K. D. Proton-conducting Oxides. *Annu. Rev. Mater. Res.* **2003**, *33*, 333–359.
- (7) Group, L.; Anderson, H. U. Densification of La<sub>1-x</sub>Sr<sub>x</sub>CrO<sub>3</sub>. *J. Am. Ceram. Soc.* **1976**, *59*, 449–450.
- (8) Duan, C.; Tong, J.; Shang, M.; Nikodemski, S.; Sanders, M.; Ricote, S.; Almansoori, A.; O'Hayre, R. Readily Processed Protonic Ceramic Fuel Cells with High Performance at Low Temperatures. *Science* **2015**, *349*, 1321–1326.
- (9) Mu, S.; Zhao, Z.; Lei, J.; Hong, Y.; Hong, T.; Jiang, D.; Song, Y.; Jackson, W.; Brinkman, K. S.; Peng, F.; Xiao, H.; Tong, J. Engineering of Microstructures of Protonic Ceramics by a Novel Rapid Laser Reactive Sintering for Ceramic Energy Conversion Devices. *Solid State Ionics* **2018**, *320*, 369–377.
- (10) Coors, W. G.; Manerbin, A.; Martinefski, D.; Ricote, S. Fabrication of yttrium-doped barium zirconate for high performance protonic ceramic membranes. *Perovskite Nanomaterials—Synthesis*,

*Characterization, and Applications*; IntechOpen Limited: London, U.K., 2016; pp 83–106.

(11) Will, J.; Mitterdorfer, A.; Kleinlogel, C.; Perednis, D.; Gauckler, L. J. Fabrication of Thin Electrolytes for Second-Generation Solid Oxide Fuel Cells. *Solid State Ionics* **2000**, *131*, 79–96.

(12) Loureiro, F. J. A.; Nasani, N.; Reddy, G. S.; Munirathnam, N. R.; Fagg, D. P. A review on sintering technology of proton conducting BaCeO<sub>3</sub>–BaZrO<sub>3</sub> perovskite oxide materials for Protonic Ceramic Fuel Cells. *J. Power Sources* **2019**, *438*, 226991.

(13) Wang, X.-H.; Deng, X.-Y.; Bai, H.-L.; Zhou, H.; Qu, W.-G.; Li, L.-T.; Chen, I.-W. Two-step sintering of ceramics with constant grain-size, II: BaTiO<sub>3</sub> and Ni–Cu–Zn Ferrite. *J. Am. Ceram. Soc.* **2006**, *89*, 438–443.

(14) Wang, X.-H.; Chen, P.-L.; Chen, I.-W. Two-step sintering of ceramics with constant grain-size, I. Y<sub>2</sub>O<sub>3</sub>. *J. Am. Ceram. Soc.* **2006**, *89*, 431–437.

(15) Durán, P.; Capel, F.; Moure, J. A strategic two-stage low-temperature thermal processing leading to fully dense and fine-grained doped-ZnO varistors. *Adv. Mater.* **2002**, *14*, 137–141.

(16) Wang, S.; Zhang, L.; Zhang, L.; Brinkman, K.; Chen, F. Two-step sintering of ultrafine-grained barium cerate proton conducting ceramics. *Electrochim. Acta* **2013**, *87*, 194–200.

(17) Wang, S.; Liu, Y.; He, J.; Chen, F.; Brinkman, K. S. Spark-plasma-sintered barium zirconate based proton conductors for solid oxide fuel cell and hydrogen separation applications. *Int. J. Hydrogen Energy* **2015**, *40*, 5707–5714.

(18) Dancer, C. E. J. Flash sintering of ceramic materials. *Mater. Res. Express* **2016**, *3*, 102001.

(19) Cologna, M.; Prette, A. L. G.; Raj, R. Flash-sintering of cubic yttria-stabilized zirconia at 750°C for possible use in SOFC manufacturing. *J. Am. Ceram. Soc.* **2011**, *94*, 316–319.

(20) Liu, F.; Gong, M. *Nano-Scaled Grain Growth Sintering RHR Castro and Kvan Benthem*, 1st ed.: Springer: Berlin, 2013; pp 35–55.

(21) Tong, J.; Clark, D.; Hoban, M.; O'Hayre, R. Cost-effective solid-state reactive sintering method for high conductivity proton conducting yttrium-doped barium zirconium ceramics. *Solid State Ionics* **2010**, *181*, 496–503.

(22) Vlajić, M. D.; Bhattacharjee, S.; Krstić, V. D. Synthesis, Sintering and Properties of Doped LaSrCrO<sub>3</sub>. *Mater. Sci. Forum* **2009**, *413*, 121–128.

(23) Manthiram, A.; Bourell, D. L.; Marcus, H. L. Nanophase Materials in Solid Freeform Fabrication. *J. Occup. Med.* **1993**, *45*, 66–70.

(24) Xiao, H.; Tong, J.; Peng, F.; Brinkman, K. S.; Mu, S.; Lei, J.; Hong, Y.; Huang, H.; Bordia, R. K. Integrated Additive Manufacturing and Laser Processing Systems and Methods for Ceramic, Glass, and Silicon Carbide Application. Provisional Patent Application, No. 62/955,780, December 31, 2019.

(25) Berman, B. *Bus. Horiz.* **2012**, *55*, 155–162.

(26) Duan, C.; Hook, D.; Chen, Y.; Tong, J.; O'Hayre, R. Zr and Y Co-Doped Perovskite as a Stable, High Performance Cathode for Solid Oxide Fuel Cells Operating below 500 °C. *Energy Environ. Sci.* **2017**, *10*, 176–182.

(27) Nikodemski, S.; Tong, J.; Duan, C.; O'Hayre, R. Ionic Transport Modification in Proton Conducting BaCe<sub>0.6</sub>Zr<sub>0.3</sub>Y<sub>0.1</sub>O<sub>3-δ</sub> with Transition Metal Oxide Dopants. *Solid State Ionics* **2016**, *294*, 37–42.

(28) Cheng, S.; Wang, Y.; Zhuang, L.; Xue, J.; Wei, Y.; Feldhoff, A.; Caro, J.; Wang, H. A Dual-Phase Ceramic Membrane with Extremely High H<sub>2</sub> Permeation Flux Prepared by Autoseparation of a Ceramic Precursor. *Angew. Chem. Int. Ed.* **2016**, *55*, 10895–10898.

(29) Hong, Y.; Lei, J.; Heim, M.; Song, Y.; Yuan, L.; Mu, S.; Bordia, R. K.; Xiao, H.; Tong, J.; Peng, F. Fabricating Ceramics with Embedded Microchannels Using an Integrated Additive Manufacturing and Laser Machining Method. *J. Am. Ceram. Soc.* **2019**, *102*, 1071–1082.